AVCO EVERETT

RESEARCH LABORATORY

a division of
AVCO CORPORATION

FINAL PROGRESS REPORT

Contract No. NASw-748

July 1965

prepared for

HEADQUARTERS
NATIONAL AERONAUTICS AND SPACE ADMINISTRATION
OFFICE OF ADVANCED RESEARCH AND TECHNOLOGY
Washington, D. C.

FINAL PROGRESS REPORT

prepared by

AVCO-EVERETT RESEARCH LABORATORY
a division of
AVCO CORPORATION
Everett, Massachusetts

Contract No. NASw-748

July 1965

prepared for

HEADQUARTERS
NATIONAL AERONAUTICS AND SPACE ADMINISTRATION
OFFICE OF ADVANCED RESEARCH AND TECHNOLOGY
Washington, D.C.

I. KRAMER'S RADIATION

1. Apparatus and Procedure

The present measurements of Kramer's radiation were made behind incident and reflected shocks in an electric-arc driven shock tube having a driven section 30 feet long by 6 inches in diameter. Most of the data were taken behind reflected shock in air at an initial pressure of 1 mm Hg for which the experimental test time varied between 10 and 30 μsec.

The continuum radiation measurements were made in two wavelength regions. The earlier measurements were made at 5100 Å since this region was relatively free of other sources of radiation as determined from incident shock spectra while the more recent measurements were made at 3250 Å where the theory based on a hydrogen-like model may possibly break down.

The instrument used was a Jarrell-Ash grating monochrometer equipped with three 6291 photomultipliers for the measurements at 5100 Å. The middle channel measured the radiation at the wavelength selected by the monochrometer $\pm$ 25 Å while the "red" and "blue" channels measured the radiation at 50 $\pm$ 25 Å above and below that selected by the monochrometer, respectively. For the measurements at 3250 Å, we used a single 6903 photomultiplier with the monochrometer for which the spectral resolution was $\pm$ 50 Å. In addition, a filter which cut off at 3500 Å was used to reduce the effects of scattered light.

In each wavelength region, the entire optical system was periodically calibrated as a unit using a standard tungsten ribbon filament lamp which was calibrated by the National Bureau of Standards. In addition, the windows

at the test section were cleaned following each run to eliminate variations in transmission as a result of the accumulation of by-products from the driver. This was found to be a significant factor under the reflected shock conditions, particularly at temperatures above 11,000°K.

2. Experimental Results

Most of our experimental measurements of Kramer's radiation were made in the vicinity of 5100 Å in both air and pure nitrogen behind incident and reflected shocks. Figures 1 and 2 show the results of our measurements behind reflected shock in air and nitrogen, respectively. The black body curve shown in each figure is based on the path length (~7 cm) across the test section. It indicates that the gas sample is nearly black at the higher velocities and that self-absorption is becoming important. The curves labeled "N^+_{fb+ff}" are for an optically thin gas while the curves labeled "total" include the effects of self-absorption. Figure 3 shows the results of measurements made in nitrogen at an equilibrium temperature of 9250°K over a range of densities. The various theory lines will be discussed below.

Figure 4 shows the results of measurements behind reflected shocks in air at a wavelength of 3250 ± 50 Å. Here again the black body curve is based on the path length across the test section. Both the "N^+_{fb+ff}" curve and the "total" curve include self-absorption effects.

3. Analysis

A calculation procedure was developed which uses the continuum oscillator strengths of Bethe and Salpeter[1] to make the free-bound radiation predictions for comparison with the measurements reported in the previous section of this report. This calculation procedure is briefly described in Ref. 2 and procedes as follows.

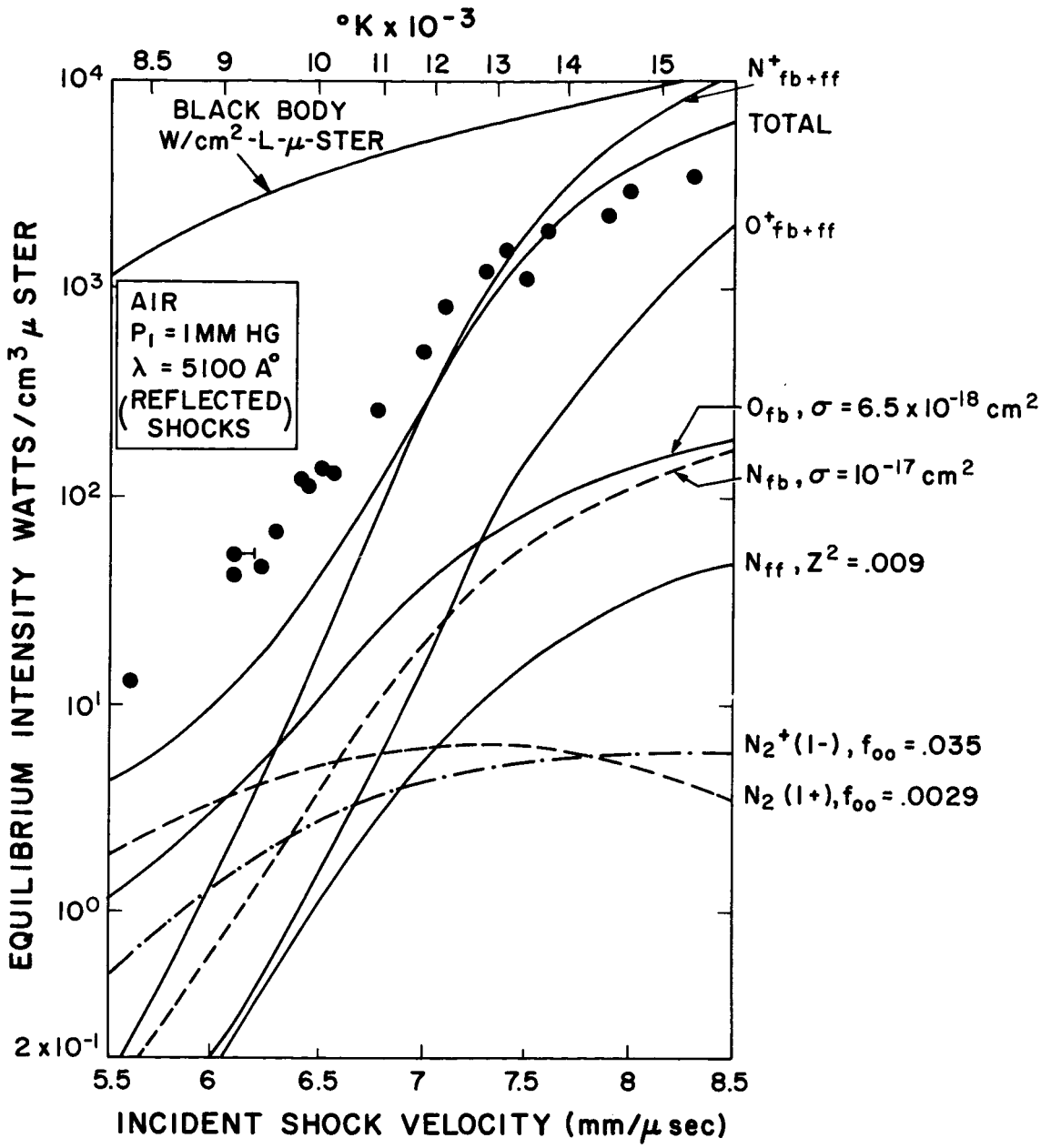

Fig. 1 Photometric measurements of continuum air radiation emitted in the vicinity of 5000 Å. The data was obtained from reflected shock waves and the highest electron concentrations were of the order of 10^{18}. The theory lines are discussed in the text.

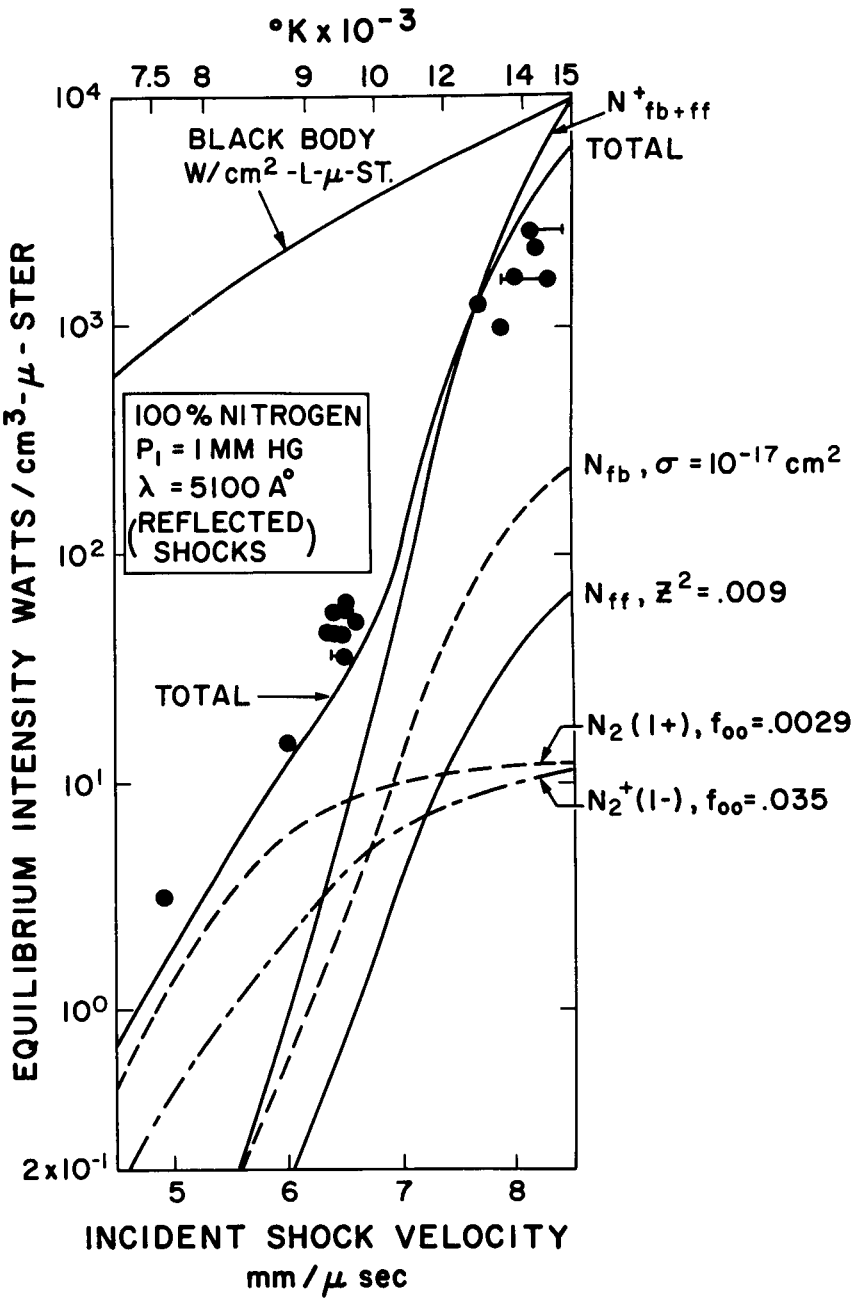

Fig. 2 Photometric measurements of the continuum radiation emitted from nitrogen.

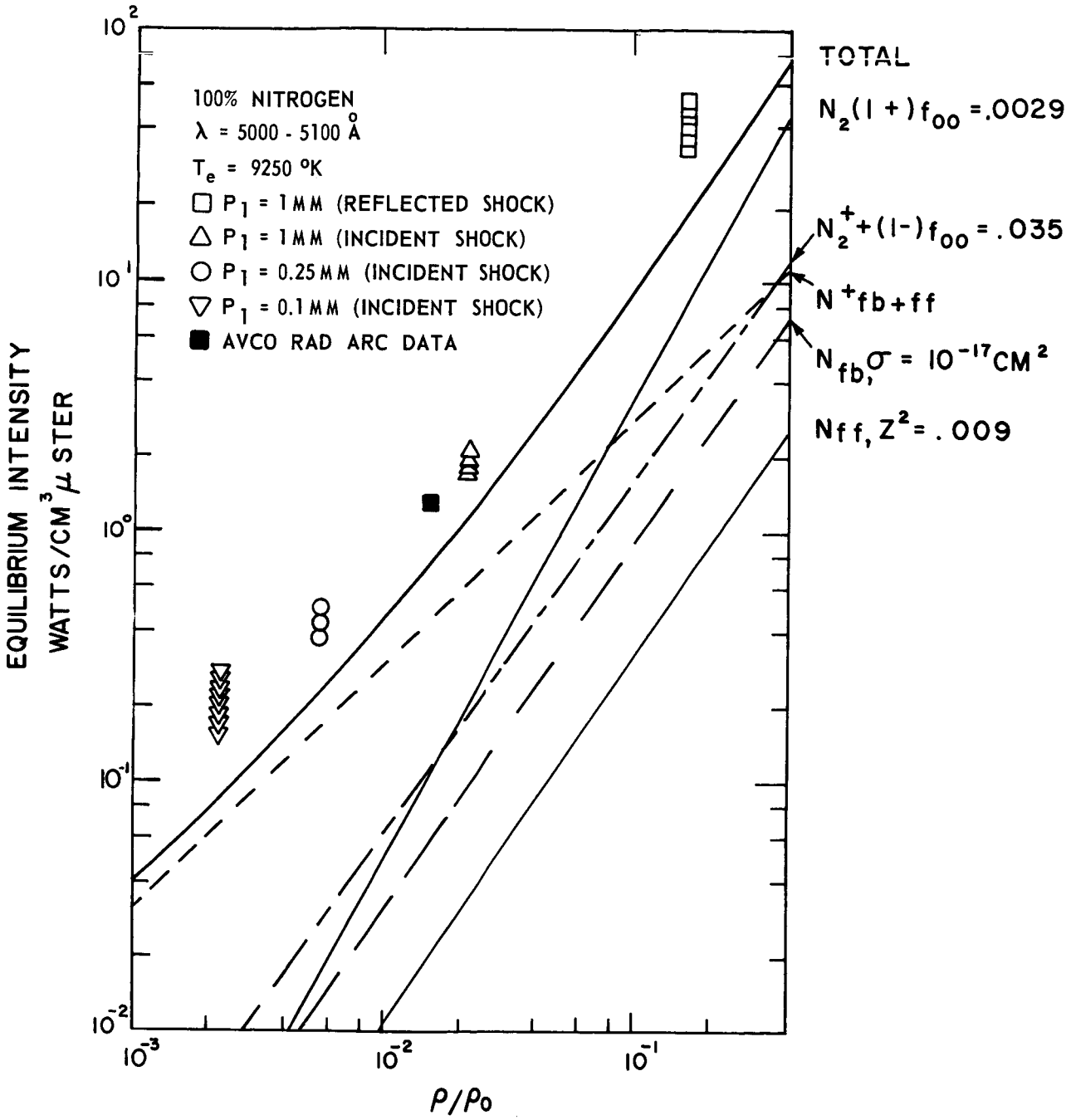

Fig. 3 Photometric measurements of equilibrium nitrogen at 9250°K in the vicinity of 5100 Å behind incident and reflected shock waves. The pertinent parameters for calculating the various contributors to the radiation are written in the right-hand margin. The N_{fb}^+ calculation is discussed in the text.

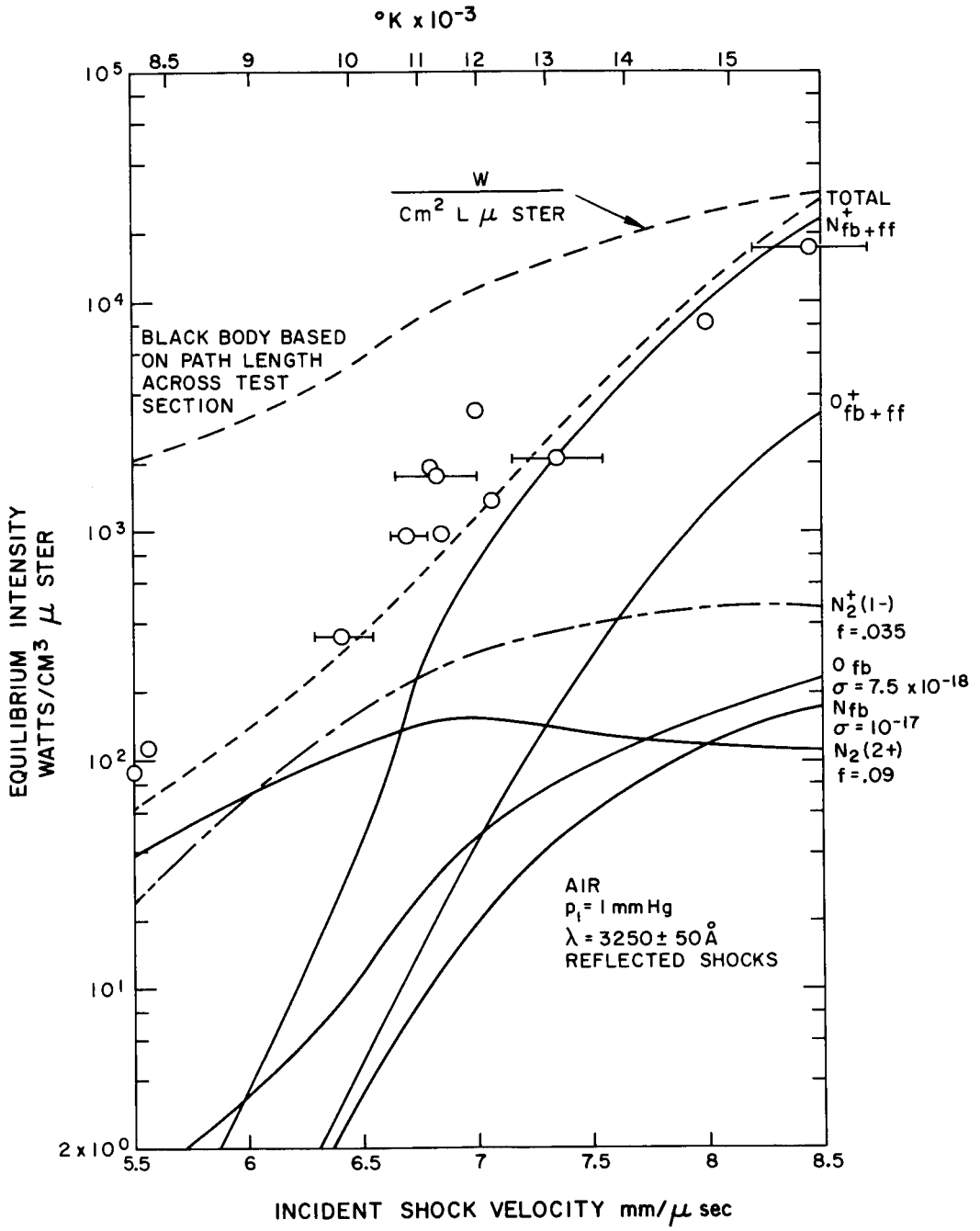

Fig. 4 Photometric measurements of the equilibrium radiation at 3250 Å behind reflected shock waves in air. The theory lines are discussed in the text.

The classical wave number dependence for a hydrogen photoabsorption edge is $\frac{1}{\tilde{\nu}^3}$. The f sum rule also states that $\int \sigma d\tilde{\nu} = \pi r_o f$ where r_o is the classical electron radius and f is the oscillator strength. Therefore,

$$\sigma = \pi r_o^2 \frac{\tilde{\nu}_{n\ell}^2}{\tilde{\nu}^3} \bar{f}_{n\ell} \qquad (1)$$

where $\tilde{\nu}^2$ is the wave number of the photoabsorption edge of atomic state n, ℓ and $\bar{f}_{n\ell}$ is the continuum oscillator strength of state of principal quantum number, n, and azimuthal quantum number, ℓ. Energy levels can be taken from tables such as Moore's[4] to locate the position of photoabsorption edges. The continuum oscillator strengths in conjunction with equation (1) can be used to obtain the photoabsorption cross section for each level of the atom versus wave number. Contributions from all levels can then be summed. Bethe and Salpeter provide the continuum oscillator strengths for all n states less than 5, and for all other states the following expression can be used with the constraint that $\bar{f}$ must be equal to or less than 1.

$$\bar{f} = \frac{16 R^2}{3\sqrt{3}\pi \tilde{\nu}_{n\ell}^2 (2J+1) n^3} \qquad (2)$$

Formula (2) can be obtained from the usual expression for the free-bound cross absorption cross section for hydrogen[5] and equation (1). $\tilde{\nu}_{n,\ell}$ is the wave number of the photoabsorption edge for a given state. J and n are the inner and principle quantum numbers, respectively. R is the Rydberg expressed in wave numbers.

From the photoionization cross section, the radiation emitted from an equilibrium gas sample of thickness L perpendicular to the surface is given by

$$\frac{dI}{dA d\tilde{\nu} d\Omega} = BB_{\tilde{\nu}_\perp} (1-e^{-\sigma_{n,\ell} N_{n,\ell} L}) (1-e^{-hc\tilde{\nu}/kT}) \qquad (3)$$

If the gas is optically thin, the resultant expression for the radiation per unit volume becomes

$$\frac{dI}{dV\,d\tilde{\nu}\,d\Omega} = N_{n,\ell}\,\sigma_{n,\ell}\,BB_{\tilde{\nu}\perp}\,(1-e^{-hc\,\tilde{\nu}/kT}) \qquad (4)$$

$BB_{\tilde{\nu}\perp}$ is the black body intensity perpendicular to the surface and $(1-e^{-hc\,\tilde{\nu}/kT})$ is the factor which properly accounts for induced emission. h and c are the usual constants. $N_{n,\ell}$ is the concentration of absorbing atoms in state n,ℓ and $\sigma_{n,\ell}$ is the photoabsorption cross section of state n,ℓ. A computer program was written to calculate the free bound radiation from optically thin samples of N^+ and O^+ using the procedure outlined above. Typical results are shown in Fig. 5 for the N^+ radiation per total number of neutral N atoms for 9650°K. Also shown in the figure are the free-free and total radiation using the Unsold expression with an effective Z^2 of 1.

The theory lines for the N^+ and O^+ free-bound radiation in Figs. 1-4 were calculated using Eq. 4. By applying the factor $(1-e^{-\sigma_n,\ N_{n,\ell}\ L})$ from Eq. 3, one can correct for the effects of self-absorption. The f number used for the N_2 (1+) system is that which corresponds to an electronic transition moment of 0.1 as indicated from the data presented in Ref. 6. No wave length dependence for the transition moment is assumed. This is in accord with the recent work of Brennen[7]. The f number used for the N_2^+ (1-) system of .035 is fairly well established[8,9] as the correct value and again no wave length dependence is assumed for the electronic transition moment. A photoabsorption cross section of 10^{-17} cm^2 is used in order to estimate the N^- continuum. The nitrogen data can be seen to be adequately fit by using these various oscillator strengths and the hydrogen model for the radiation. The effective Z^2 used for the N^+ and O^+ free-free components

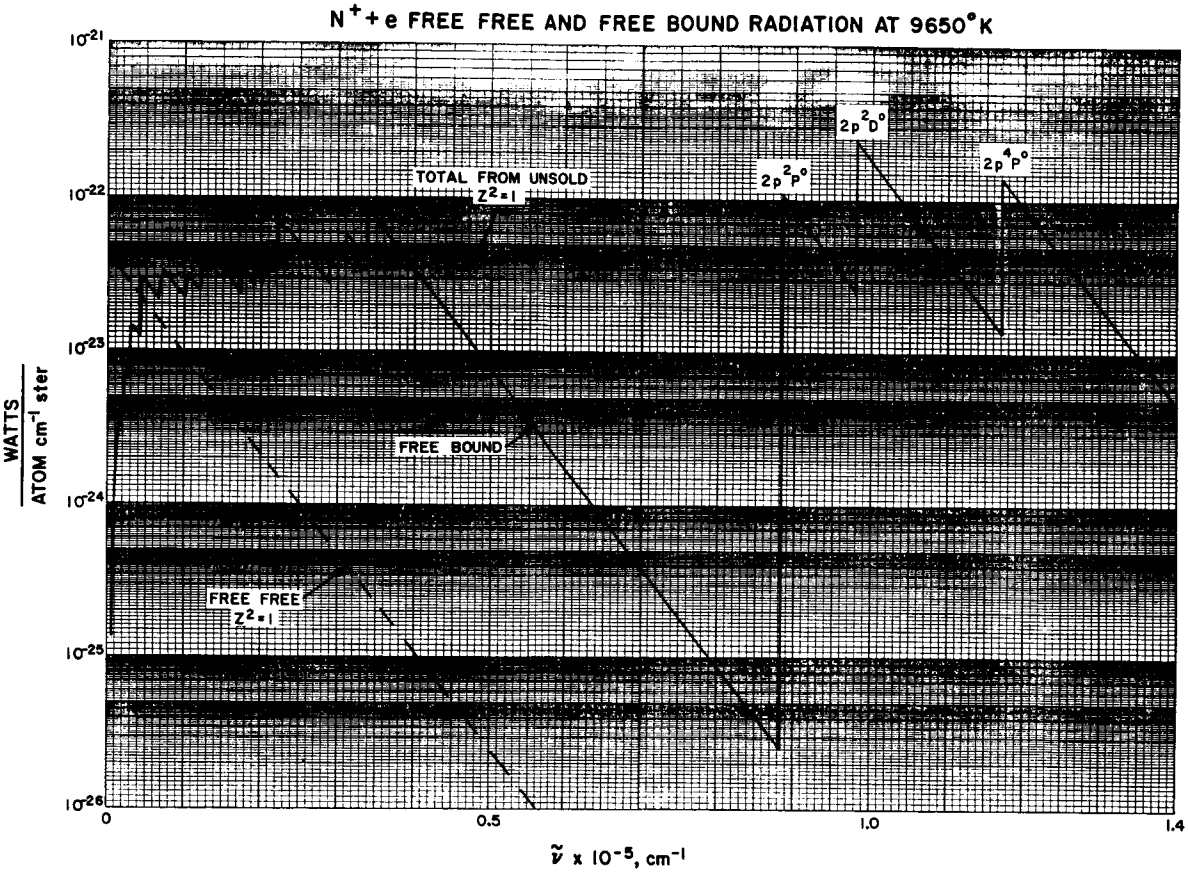

Fig. 5 Free-bound calculations at 9650°K using the hydrogen-like model for the nitrogen atom described in the text. The 2p states are most likely to be in error using this model. An Unsöld calculation for the total and free-free radiation using an effective Z^2 of 1 is also plotted.

of the radiation is 1.5 in accord with the infrared data reported in Ref. 2. The Z^2 for N_2 free-free is that measured by Taylor.[10] At the high temperature end of the data the dominant form of radiation is that from N^+ and O^+ and these measurements serve as a good check on the free bound theory. At these high electron concentrations the gas is partially black and the theory plotted in Figs. 1, 2 and 4 for the total radiation includes self-absorption. It is seen in both the nitrogen and air data that the free bound theory line is higher than the measurements by about 50%. In general, however, the high temperature data is adequately fit by the hydrogen-like model for the free bound radiation.

At the lower temperature end of the data the nitrogen measurements are in good agreement with predictions while in air they are higher than the measurements by about a factor of two. This anomalous behavior for air has been observed before[6] and as yet there is no satisfactory explanation. This is particularly true for the data taken at 5100 Å while the data at 3250 Å agree more closely with theory over the temperature range between 10,000 and 15,000°K. No comparative measurements have been made in pure nitrogen at 3250 Å at this time.

4. Comparison of Shock Tube and Arc[11] Data

Morris of Avco/RAD has been making extensive measurements in a wall stabilized arc of the radiation emitted from a nitrogen plasma. In general his measurements and our shock tube data agree very well. Figure 6 shows measurements of Morris at 5000 Å over a range of temperatures. The theoretical lines are based on the same theories as those used to construct the theory lines for the nitrogen shock tube data of.Fig. 2. The temperature dependence of the data is very well fit by the combination of the free-bound radiation and the N_2^+ (1-) and N_2 (1+) molecular bound systems.

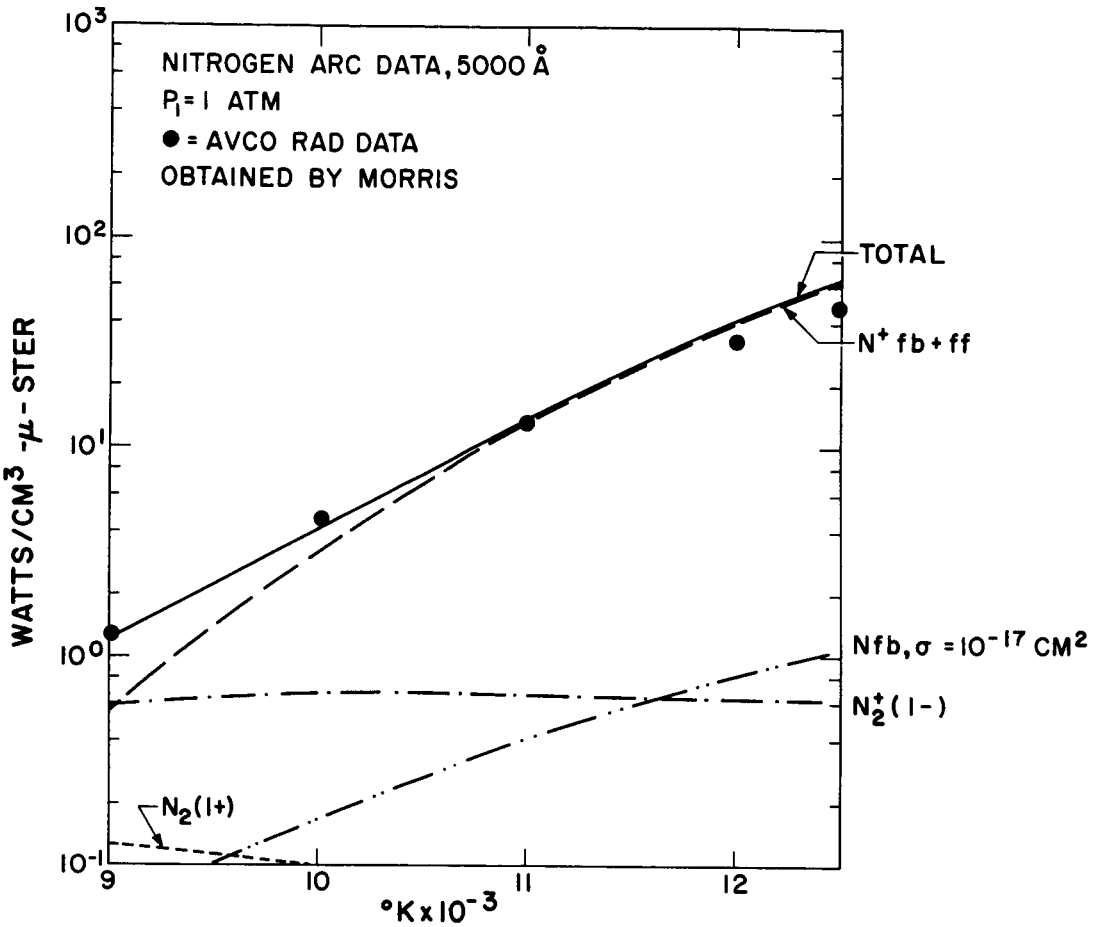

Fig. 6 Nitrogen arc data obtained by Morris at Avco/RAD. The theory lines are constructed using the same constants as those used to draw the theory lines in Fig. 2. This figure in conjunction with the theory curves and Fig. 2 serve to show the very good agreement between the arc and shock tube data.

The contributions from the molecular bound systems were calculated using a smeared rotational line model for the radiation.[9]

A wavelength comparison of the arc data and a theoretical free-bound prediction is shown in Fig. 7. The apparent shift in photoelectric edges due to electron concentration was not taken into account. Also shown in the figure are the theory lines to the free-free component of the radiation using a $Z^2 = 1.5$ as determined by the previous infra-red work of Wilson[2]. An Unsold calculation with $Z = 1$ is also shown for comparison. The hydroken-like model for the N^+ ion gives poor agreement with the arc data in the ultraviolet. It will be recalled, however, that the shock tube data of Fig. 4 show very good agreement with the hydrogen-like theory in the U.V. This apparent disagreement between the arc and shock tube experiments requires further investigation.

The excess radiation measured in the near infrared is not unexpected since in this region nitrogen atomic lines are prominent and the measurements of the continuum probably have a component which is due to the wings of lines.

5. Summary

Measurements have been made of the continuum radiation in air and nitrogen from two narrow wavelength regions at 5100 Å and 3250 Å. These data agree quite well with theory when one includes the contributions from all the known radiators in each wavelength region. The air data at 5100 Å are about a factor of 2 higher than theory at the lower temperatures which could possibly be due to our using f numbers for the N_2 (1+) and N_2^+ (1-) band systems which are too low. At the high temperature end, radiative cooling may be causing the experimental data to fall below theory. A theory for the Kramer's radiation which assumes a hydroken-like model for the N^+ ion and the f numbers of Bethe and Salpeter[1] adequately predicts the Kramer's

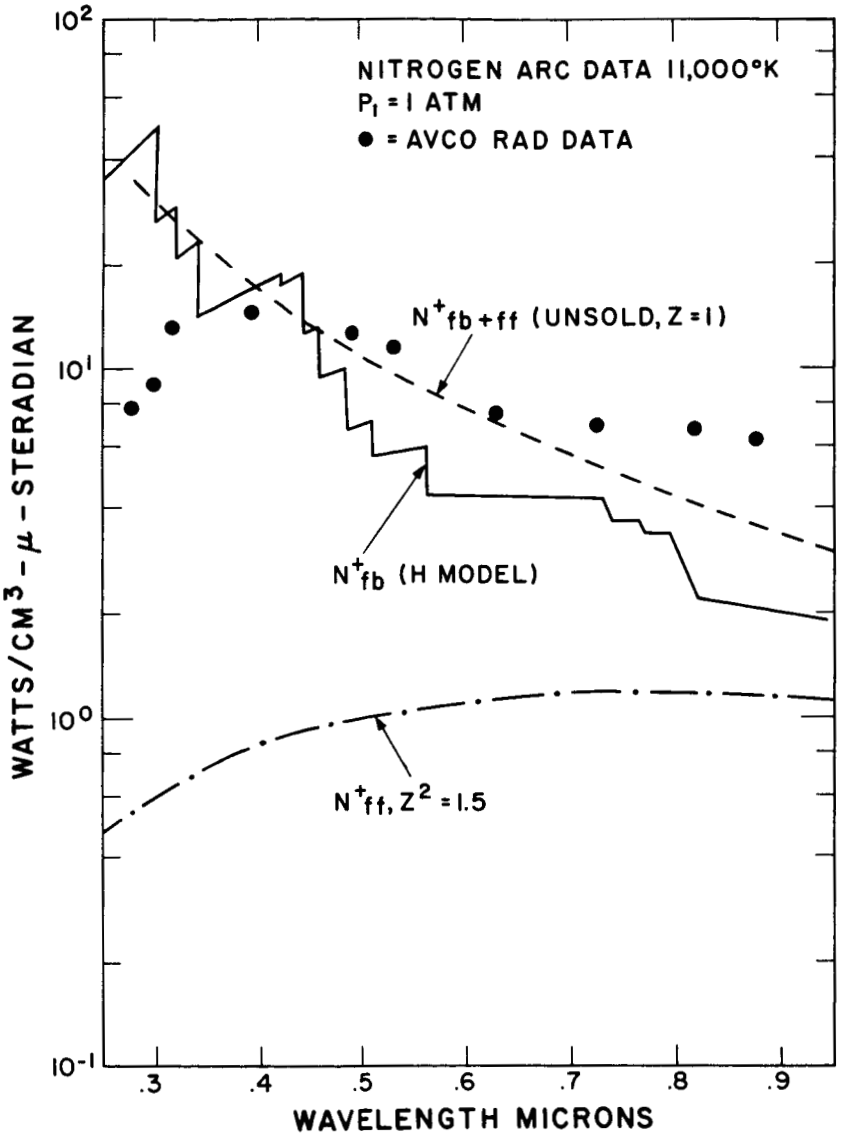

Fig. 7 Arc measurements of the continuum radiation obtained by Morris at 11,000°K as a function of wavelength and a comparison with theoretical predictions for the radiation using a hydrogen-like model. The disagreement between theory and data is in the ultraviolet.

contribution to the radiation in both of the wavelength regions covered by the shock tube experiments as well as by the arc experiments at 5000 Å.

In conclusion, we find that our shock tube data and the arc data of Morris[11] agree although our interpretation of the data is different. On the basis of our measurements, we cannot accurately assign a photo-absorption cross-section to the N^- ^1D ion. For the purpose of generating theoretical estimates of this continuum, however, we have assigned a cross section of 10^{-17} cm^2 in the vicinity of 5000 Å. It seems unlikely that the cross section is much greater than 10^{-17} cm^2 as can be deduced by invoking the f sum rule.[5]

REFERENCES

1. Bethe, H.A. and Salpeter, E.E., Quantum Mechanics of One and Two Electron Atoms, (New York, Academic Press, 1957).

2. Allen, R.A., Textoris, A. and Wilson, J., "Measurements of the Free-Bound and Free-Free Continua of Nitrogen, Oxygen and Air," Avco-Everett Research Laboratory Research Report 195, September 1964.

3. Finkelnburg, W. and Peters, T., "Kontinuierliche Spektren," Handbuch der Physik, Vol. 28 (Springer-Verlag, 1957) p. 79.

4. Moore, C.E., "Atomic Energy Levels," U.S. National Bureau of Standards Circular 467, June 1947.

5. Aller, L.H., Astrophysics: The Atmospheres of the Sun and Stars, (New York, Ronald Press, 1953) p. 146.

6. Keck, J.C., Allen, R. A. and Taylor, R.L., "Electronic Transition Moments for Air Molecules," J. Quant. Spectr. Rad. Transfer 3, 335 (1963); also Avco-Everett Research Laboratory Research Report 149, March 1963.

7. Brennen, W.R., "Studies on Active Nitrogen," Ph.D. Thesis, Harvard University, Department of Chemistry, September 1964.

8. Bennet, R.G. and Dalby, F.W., "Experimental Determination of the Oscillator Strength of the First Negative Bands of N_2^+," J. Chem. Phys. 31, 435 (1959).

9. Allen, R.A., "Nonequilibrium Shock Front Rotational, Vibrational and Electronic Temperature Measurements," Avco-Everett Research Laboratory Research Report 186, August 1964.

10. Taylor, R.L., "Continuum Infrared Radiation from High Temperature Air and Nitrogen," Avco-Everett Research Laboratory Research Report 154, May 1963; also J. Chem. Phys. 39, 2354 (1963).

11. Avco Corporation, Research and Advanced Development Division, "Research on Radiation from Arc-Heated Plasmas," Quarterly Progress Report No. 6, March-June 1963, Contract AF 33(616)-8390, June 1963.

II. ATOMIC LINE RADIATION

1. Apparatus and Procedure

The basic instrument used in measuring atomic line radiation is a triple channel Jarrel-Ash grating monochromator having a band pass of 50 Å in each channel with approximately 50 Å separation between channels. For the present measurements, the instrument was modified to reduce the band pass to 16 Å. The modified monochromator was calibrated for wavelength and band pass using both mercury and neon lamps. The measured wavelength was found to agree with the monochromator setting to within 2 Å.

The entire optical system was periodically calibrated as a unit using a standard tungsten ribbon filament lamp calibrated by the National Bureau of Standards. The spectral intensity of the lamp was calculated using data on the emissivity of tungsten given by DeVos[1] and the transmission of the quartz envelope. Filters were used to cut off the radiation below 5000 Å to prevent overlapping of orders. The quartz windows in the shock tube were thoroughly cleaned after each run to eliminate variations in transmission as a result of the accumulation of by-products from the driver.

The present measurements were made using an arc driven shock tube having a low pressure section 30 feet long and 6 inches in diameter. Shock velocities were measured by using photomultipliers to observe the radiation from the shock as it passed a series of collimated slits along the shock tube. The outputs of the photomultipliers at the beginning and at the end of each incremental distance were displayed on dual beam oscilloscopes. Timing marks were used to provide an absolute time relationship between the two

beams of each oscilloscope. By enlarging the oscillograms obtained during a run, one could measure the time required for the shock to traverse each incremental distance to $\pm$ 0.1 μsec. The experimental test time varied from 3 to 8 μsec.

Prior to each run, the shock tube was evaculated to a pressure of less than 1 μ Hg using an oil diffusion pump. Leak rates were generally less than 1 μ Hg per minute. Bottled air, flowed through an alcohol dry ice cold trap, was used as the test gas. Initial pressure was set using an alphatron vacuum gauge and was checked using a McLeod gauge before each run. To further assure a clean gas sample, the windows were mounted in flat plates with sharp leading edges which protruded well into the shock tube. This served to eliminate boundary layer effects from the gas sample.

2. Experimental Results

Most of the measurements of atomic line radiation were made to observe the radiation from atomic nitrogen undergoing transitions from the $3p\,^4S$ level to the $3s\,^4P$ level. This particular system was chosen so that two channels of the monochromator could observe line radiation while the third channel measured the background radiation. In addition, very little radiation from impurities should be present within the band pass of the monochromator in the wavelength region.

In particular, the monochromator was set at a wavelength of 7468 Å to measure radiation from the $3p\,^4S_{3/2}$-$3s\,^4P_{5/2}$ transition. At this setting of the monochromator, the "blue" channel covered the region at 7423 $\pm$ 8 Å (which includes the $3p\,^4S_{3/2}$-$3s\,^4P_{1/2}$ transition), while the "red" channel covered the region at 7507 $\pm$ 4 Å. In the latter region, radiation should be mainly from the free-bound and free-free continua of oxygen and nitrogen.

Figure 8 shows a comparison of the equilibrium data from all three channels as a function of shock velocity for air at an initial pressure of 0.1 mm Hg. The large amount of scatter in the data at 7507 Å can be attributed to the fact that the output of the photomultiplier was extremely small which made it difficult to accurately measure the equilibrium level. The data points are intended to show the relative magnitude of the background radiation with respect to the line radiation rather than to give the absolute value of this radiation. Figure 9 gives a comparison of the radiation from the $3p\,^4S_{3/2}$-$3s\,^4P_{5/2}$ atomic transition (7468 Å) as measured using two separate channels of the monochrometer. By setting the monochrometer at 7513 Å, this transition fell within the band pass of the "blue" channel. The theory lines in Figures 8 and 9 will be discussed below.

3. Analysis

The total intensity of an optically thin spectral line emitted per steradian per unit volume at thermodynamic equilibrium is

$$\frac{I}{d\,V\,d\,\Omega} = \left[N_{n,\ell}\right] \pi f\, r_o\, BB_{\tilde{\nu}\perp}(1-e^{-hc\,\nu/kT}) \qquad (1)$$

where $N_{n,\ell}$ is the number of atoms per unit volume in the absorbing state for the transition, f is the absorption bound-bound oscillator strength, r_o is the classical electron radius, $BB_{\tilde{\nu}\perp}$ is the blackbody intensity perpendicular to the surface and $(1-e^{-hc\,\tilde{\nu}/kT})$ is the induced emission term.

In many situations, atomic line transitions undergo a certain amount of self-absorption which reduce the measured total intensity from the completely optically thin situation. In order to calculate the self-absorption, one must know the principle broadening mechanism in the gas. The line width and shape are the pertinent parameters which must be known. Lines

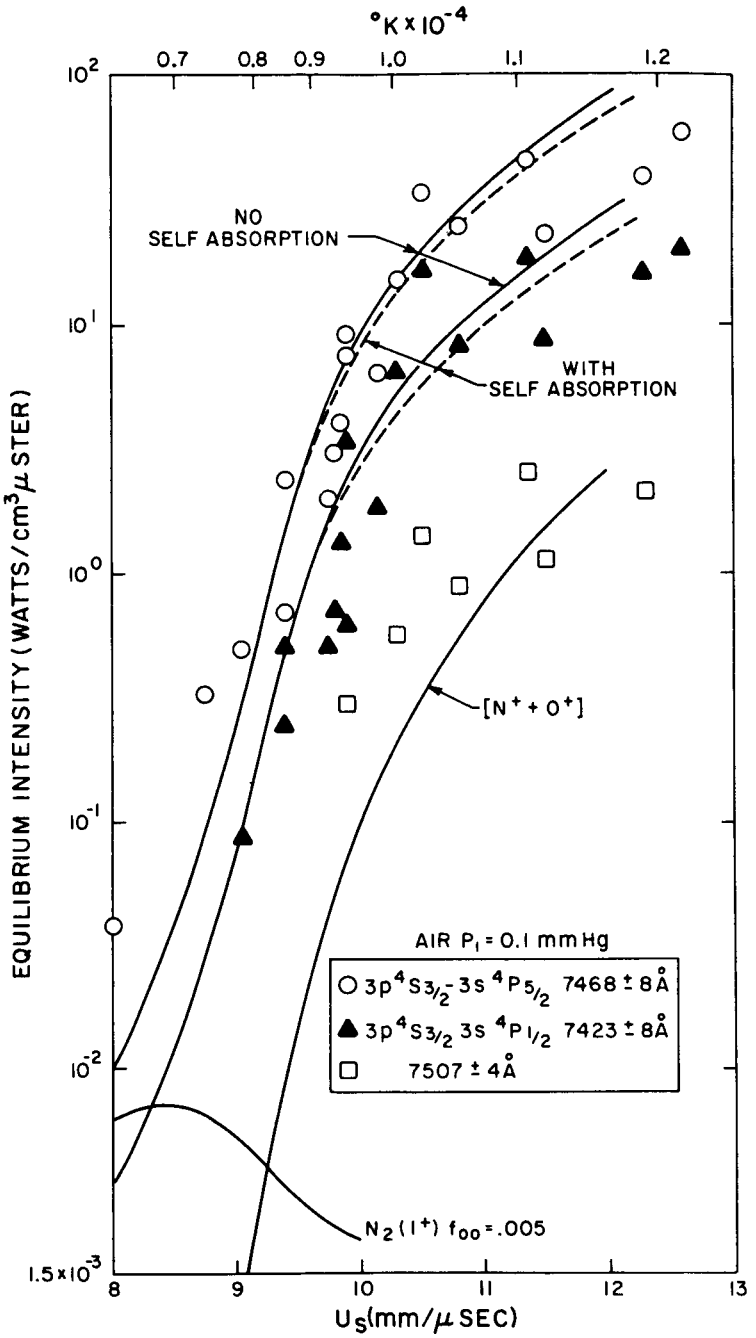

Fig. 8 Photometric measurements obtained from three wavelength channels of the equilibrium air radiation produced behind air shock waves. Two of the channels observe atomic lines while the third observes the continuum background radiation.

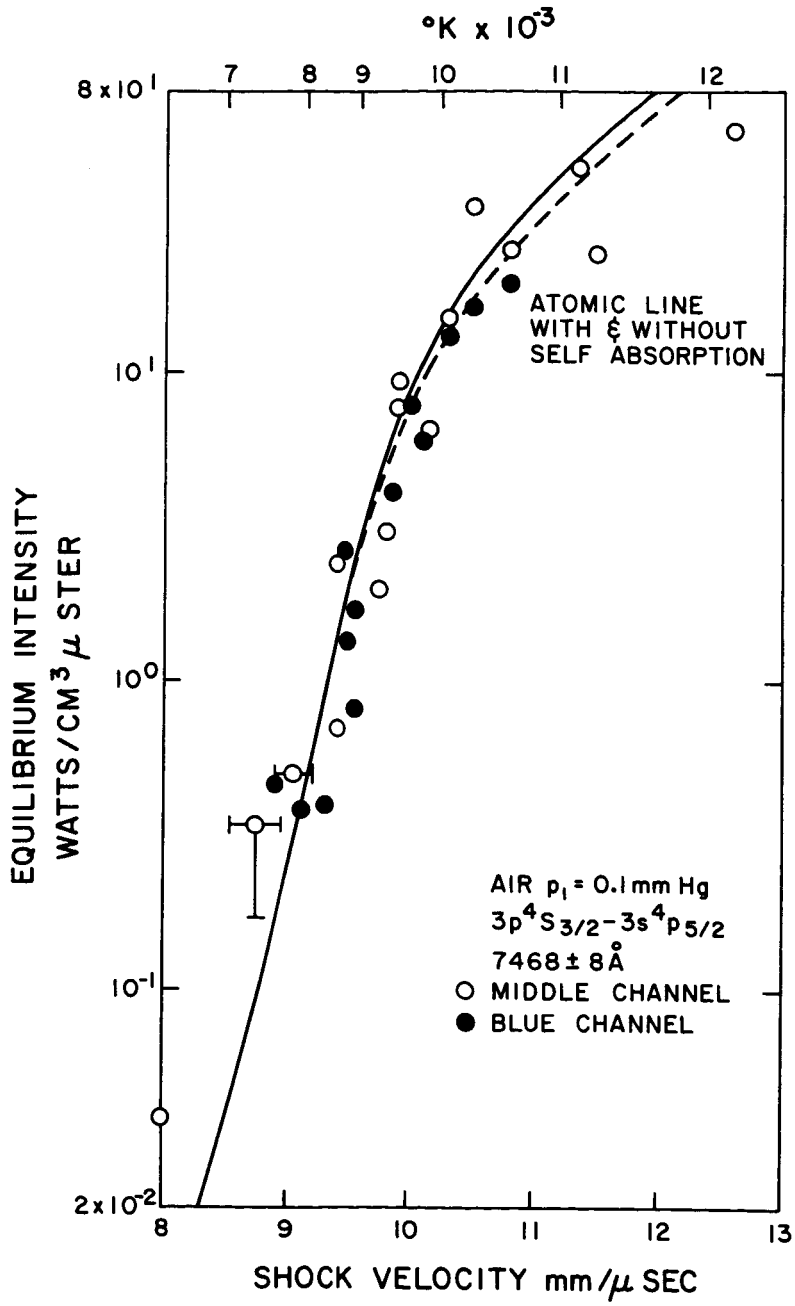

Fig. 9 Photometric measurements of the equilibrium radiation from the $3p^4S_{3/2}$ - $3s^4P_{5/2}$ atomic transition.

also undergo a small wavelength shift for certain types of broadening, however, this shift can generally be disregarded in estimating the total self-absorption of the line. For the densities and temperatures normally encountered in shock tubes, doppler and electron broadening mechanisms dominate over natural and pressure broadening by neutrals. Under the conditions of our measurements of line radiation between 9 and 12 mm/μsec, in the wavelength vicinity of .75 μ, line broadening by electron impact calculates to be the most important broadening mechanism. The electron impact width[2] at an electron concentration of 10^{16}, and a temperature of 10,000°K, calculates to be at least 10 times the doppler width at .75 μ. A good review of spectral line shape theory is given in reference 3. For our purpose, it will be adequate to assume that the principle broadening mechanism is that produced by impact of atoms with slow electrons. For estimating this effect, the electron impact formula of Armstrong[2] and Stewart and Pyatt[4] is used. The total line width in wave numbers is given by

$$W_{\tilde{\nu}} = 5.67 \times 10^{-16} N_e \frac{n^4}{Z^2} T^{-1/2} \text{ cm}^{-1} \qquad (2)$$

where N_e is the electron density, n is the principle quantum number of the upper state, Z is the total charge of the atom minus one and T is the temperature. Self-absorption of Lorentz, or dispersion shaped, non-overlapping lines, is treated in detail by various authors.[5,6] For our purposes, we have followed the definitions of Penner[5] and Plass[6] for f(x) where

$$x = \frac{\left[N_{n,\ell}\right] f r_o L}{W_{\tilde{\nu}}} =$$

$$\frac{N_{n,\ell} f r_o Z^2 T^{1/2}}{5.67 \times 10^{-16} N_T n^4} \cdot \frac{N_T}{N_e} L = K \frac{N_T}{N_e} L \qquad (3)$$

$\frac{f(x)}{x}$ is plotted versus x in Fig. 10 and is the value by which a completely optically thin calculation (equation 1) must be multiplied in order to correct for self-absorption. In expression (3), N_T is the total number of atoms and is introduced so that K is a function only of temperature for a given transition. Using equation (1) and (3) divided by the experimental band pass, and using the oscillator strengths of Richter[7], one can generate the theory curves in Figs. 8 and 9.

4. Non-Equilibrium Radiation

At shock velocities below about 10 mm/μsec (at initial pressures of 0.1 mm Hg), the radiation is observed to overshoot at the shock front followed by a decay to an equilibrium level. Figure 11 shows typical trace in each oscillogram is from the photomultipliers at 7468 Å, while the lower trace is a record of a photomultiplier at about 5000 Å. The latter photomultiplier was used to monitor test time and to compare signals in the visible and near infrared. In the oscillogram at 10.3 mm/μsec, the lower trace is that of the photomultiplier at 7423 Å. The odd signal shown in the lower trace at 12.3 mm/μsec is due to saturation of the photomultiplier and scattered light.

We have gained some information on the source of the overshoot from photometric measurements. In our earlier measurements, the channel which we used to measure the background radiation was quite weak and as a result our data from this channel cut off at about 10 mm/μsec. Because of the manner in which the photomultipliers are mounted on the monochromator, the middle channel has a much greater sensitivity than the other channels. By setting the middle channel at 7513 Å, we were able to monitor the $3p^4S_{3/2}$-$3s^4P_{5/2}$ transition at 7468 Å with the "blue" channel which enabled us to measure both the background and line radiation down to 9 mm/μsec.

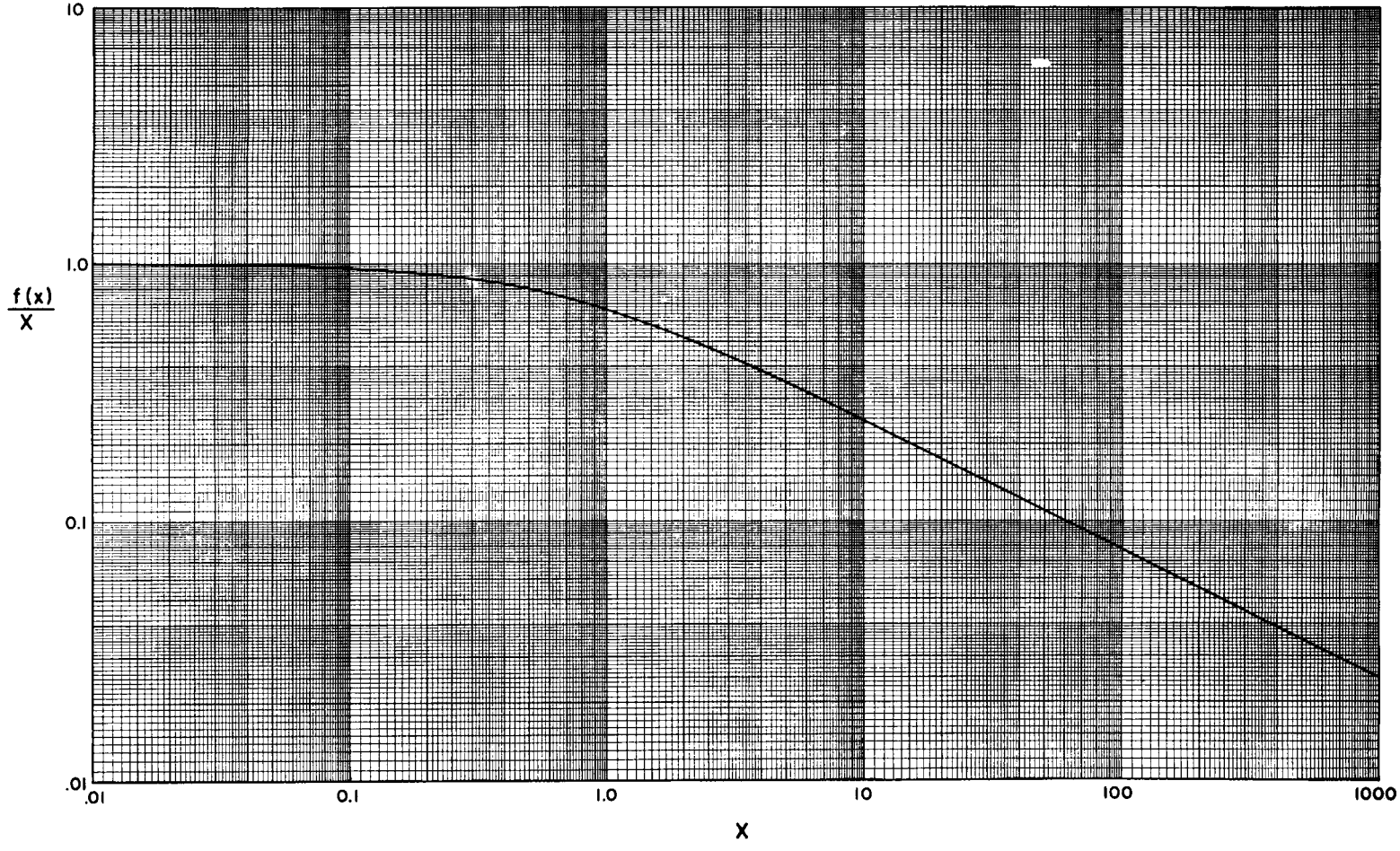

Fig. 10 f(x)/x is the factor by which a completely optically thin calculation of a dispersion shaped line must be multiplied in order to correct for self-absorption. x is defined in equation (9) of the text.

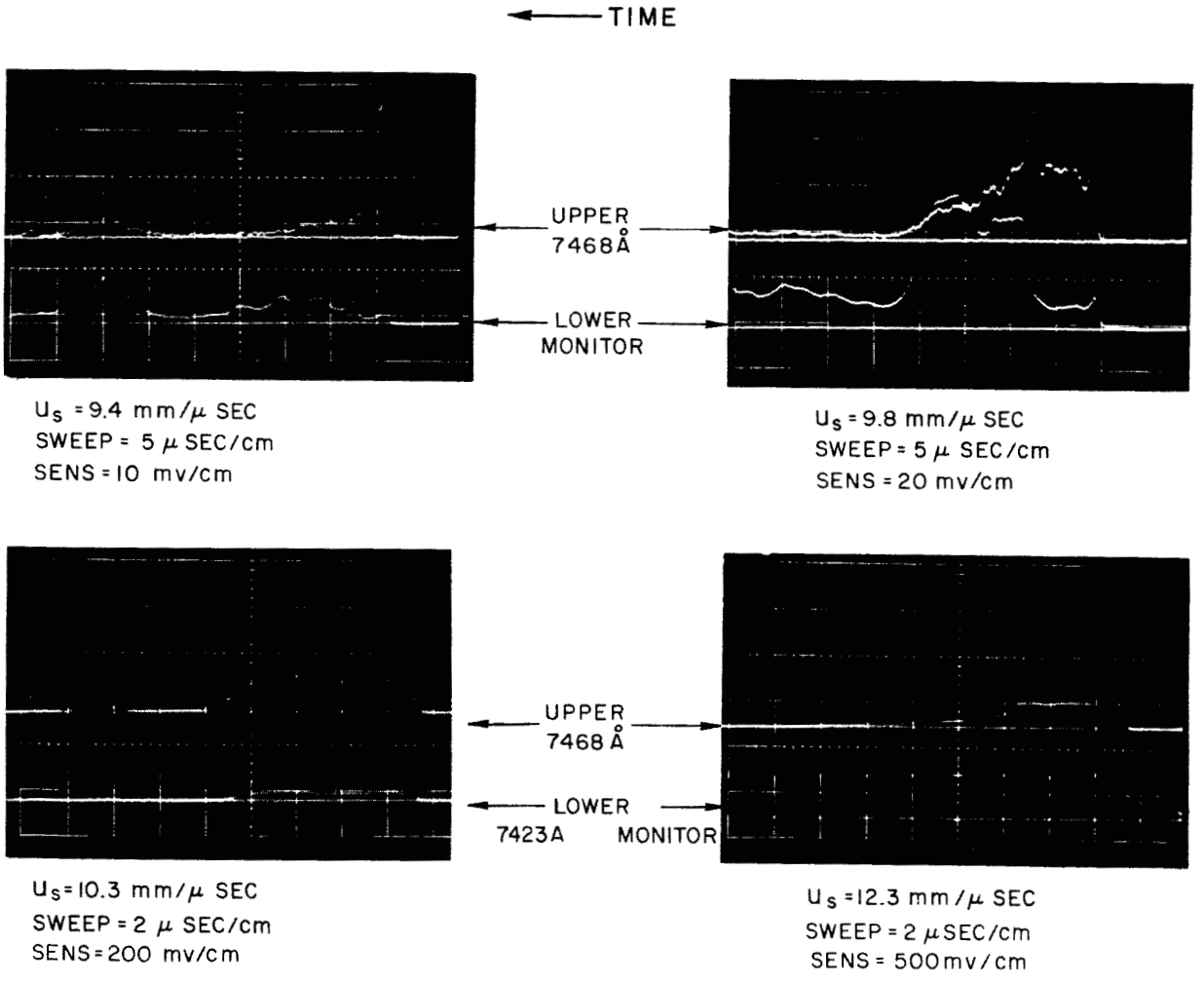

Fig. 11 Typical oscillogram traces obtained with the triple channel monochromator on incident shock waves.

The results of these measurements are shown in Fig. 12. The symbol usage is defined on the figure. The vertical bars connecting the open and closed symbols indicate that both points are from the same run. Note that the peak non-equilibrium intensities are much greater for the "line" channel than for the "background" channel. Since the distribution function for the $N_2(1+)$ band system shows that each channel should see about the same intensity and since Kramers' radiation has not been known to overshoot (even if it did both channels would see the same intensity), the measurements indicate that the overshoot is due to the nitrogen atom.

Figure 13 is a replot of the non-equilibrium portion of the previous figure. Although the peak non-equilibrium intensity of the line increases with velocity, the peak background intensity is constant within the scatter of the data. This could possibly be explained by first considering what happens under equilibrium conditions. In the case of the N_2 (1+) band system, as the temperature increases, more of the molecules are in the lower electronic state. However, since the gas is more dissociated, there are fewer molecules present so the intensity is relatively insensitive to velocity. In the case of an atomic line, as the temperature increases, the absorbing level contains a higher percentage of the atoms. As the gas becomes more dissociated, there are also more atoms so that the intensity increases with velocity until ionization becomes significant. Assuming that the non-equilibrium region behaves similarly would account for the different velocity dependence between the two sets of data in Fig. 13.

5. Summary

This has concluded our measurements of atomic line and background radiation in the vicinity of 7500 Å. In summary, our data on equilibrium atomic line radiation are in reasonably good agreement with theory as outlined in Section 3 except possibly at the higher velocities where we may be over-estimating the line broadening due to electron impact and hence underestimating

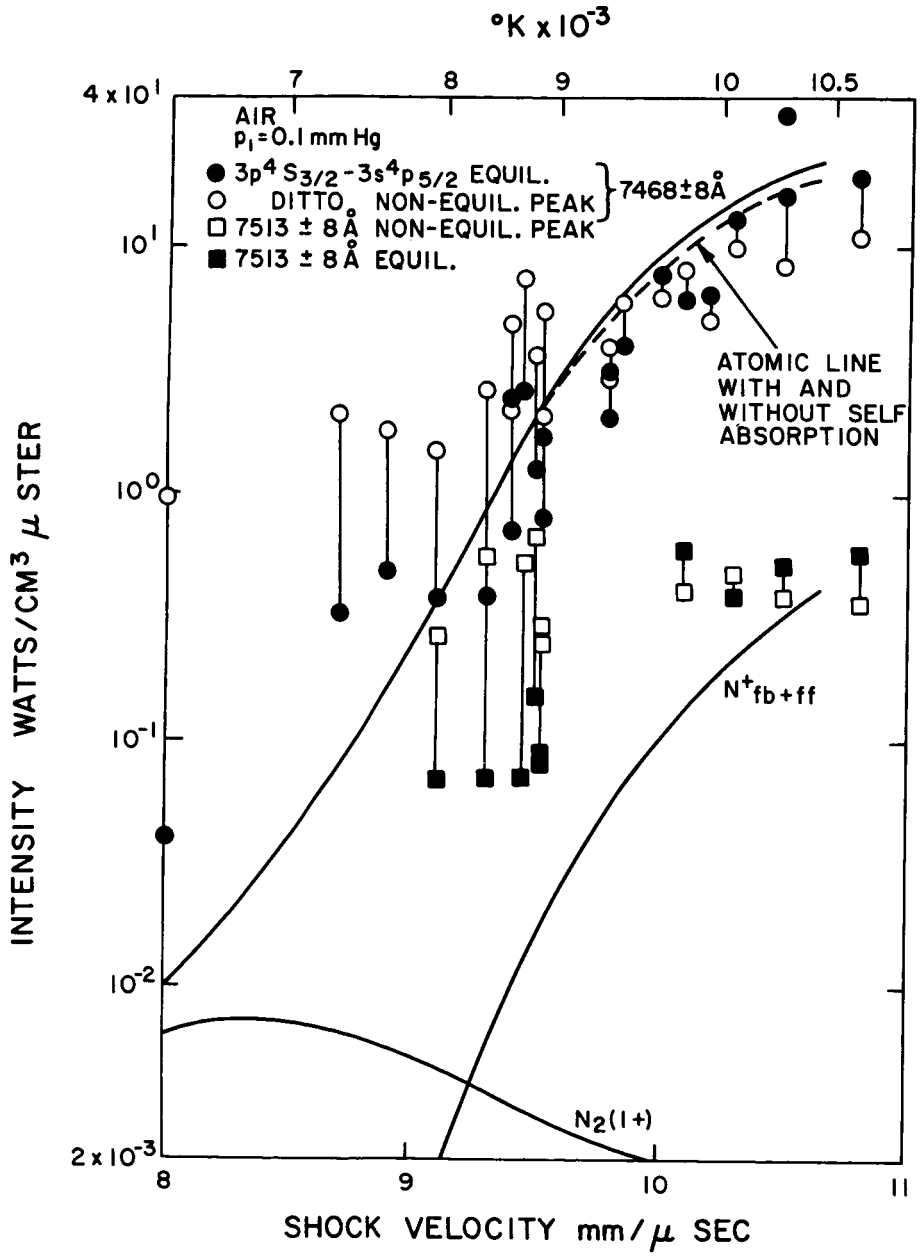

Fig. 12 Photometric measurements of atomic line and background radiation in the vicinity of 7500 Å.

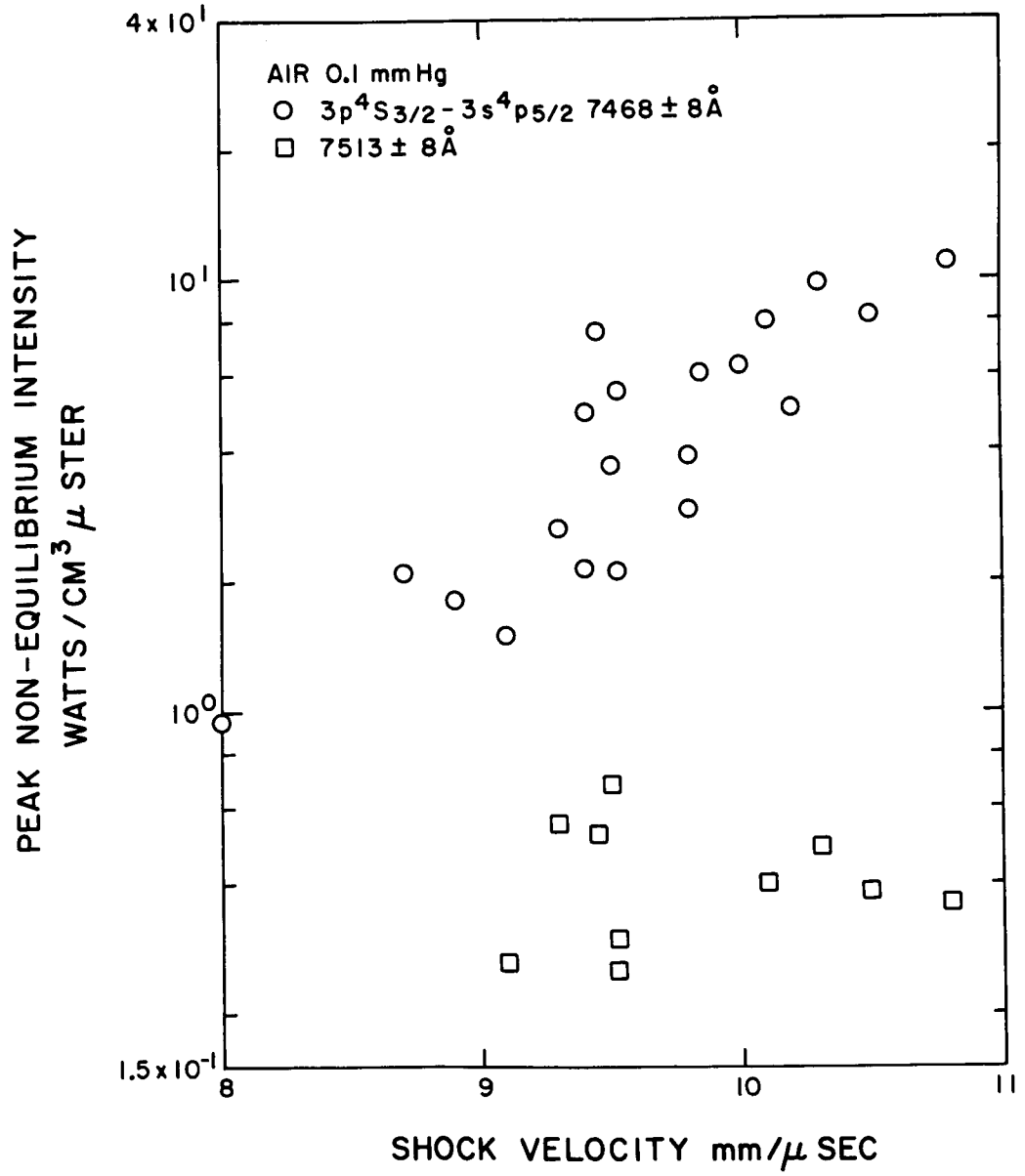

Fig. 13 Peak nonequilibrium intensity of radiation from two narrow band pass regions located at 7468 ± 8 Å and 7513 ± 8 Å. The former includes the $3p^4S_{3/2} - \bar{3}s^4P_{5/2}$ atomic transition.

the effects of self-absorption.

In addition, our data indicate that there are conditions for which the atomic line radiation overshoots at the shock front. Our contention that the lines overshoot is based on calculated intensities from the data which show the line peak intensities to be 10 to 40 times greater than that of the background as well as from the difference in the velocity dependence between the peak line intensities and the peak background intensities.

At the present time, our knowledge of both the conditions at which the lines overshoot and the atomic transitions for which an overshoot will occur are limited to one set of conditions and one transition. Additional measurements involving other transitions of the nitrogen atom as well as measurements of oxygen transitions including experiments at higher densities to test the line broadening theory are not only desirable, but necessary before one can fully understand this problem.

REFERENCES

1. DeVos, J.C., "A New Determination of the Emissivity of Tungsten Ribbon," Physica 20, 690-714 (1954).

2. Armstrong, B.H., "Broadening of Balmer Lines for High Quantum Number," J. Quant. Spectr. Rad Transf. 4, May-June 1964.

3. Barranger, M., "Spectral Line Broadening in Plasmas," in Atomic and Molecular Processes, ed. By D.R. Bates (New York and London, Academic Press, 1962) p. 493.

4. Stewart, J.C. and Pyatt, K.D., Jr., "Theoretical Study of Optical Properties. Photon Absorption Coefficients, Opacities and Equations of State of Light Elements, Including the Effect of Lines," Final Report. Contract AF 29(601)-2807, General Atomic Division, General Dynamics Corporation. September 1961.

5. Penner, S.S., Qualitative Molecular Spectroscopy and Gas Emissivities, (Addison-Wesley, 1959).

6. Plass, Gilbert N., "Models for Spectral Band Absorption," J. Opt. Soc. Amer. 48, October 1958.

7. Richter, J., "Uber Oszillator enstarken von Multipletts des neutralen Stickstoffs," Z. Astrophys 51, 177-186 (1961).

III. RADIATION TABLES

Part II of the radiation tables is completed and submitted along with this report. The abstract of these tables appears below. Part I of the radiation tables contains the spectral distribution functions and computer program output for the molecular bands. The contents of these tables is completed however have not yet been organized into a report form. This additional work will be done during the next month.

AIR RADIATION TABLES II

R. A. Allen

ABSTRACT

Calculations have been made of the equilibrium radiation emitted from air over a range of temperatues from 2,000°K to 23,000°K and over a density range from 10^{-6} to 10 atmospheres. The calculations are presented in graphical form and are in terms of the radiation flux emitted from one side of infinite slabs of finite thickness. The molecular band systems have been calculated using a smeared rotational model, and are carried out for a slab thickness of 1 cm. Atomic line and free-bound transitions are important contributors at elevated temperatures and also generally undergo significant amounts of self-absorption. Consequently calculations for these two classes of radiation have been made with slab thickness as an added parameter. The lines free bound and free-free radiation have been split into the two spectral regions for the radiation flux above and below 2000Å.